IEEE Access
Multidisciplinary ⋮ Rapid Review ⋮ Open Access Journal

Received 4 May 2025, accepted 23 May 2025, date of publication 26 May 2025, date of current version 3 June 2025.

Digital Object Identifier 10.1109/ACCESS.2025.3573900

RESEARCH ARTICLE

A Novel Fuzzy PIDF Enhancing PIDF Controller Tuned in Two Stages by TLBO and PSO Algorithms for Reliable AVR Performance

MOKHTAR SHOURAN[1,2] **AND MOHAMMED ALENEZI**[3]

[1]Libyan Centre for Engineering Research and Information Technology, Bani Waled, Libya
[2]Department of Control Engineering, College of Electronic Technology, Bani Walid, Libya
[3]School of Engineering, Cardiff University, CF10 3AT Cardiff, U.K.

Corresponding author: Mohammed Alenezi (alenezim1@cardiff.ac.uk)

ABSTRACT Reliability in control engineering remains a fundamental consideration in the design of controllers for various applications. This study proposes an innovative control design for Automatic Voltage Regulator (AVR) that integrates Fuzzy Proportional-Integral-Derivative with Filter action (Fuzzy PIDF) enhancing PIDF controllers (PIDF + Fuzzy PIDF), which is tuned in a two-stage framework. This framework leverages Teaching-Learning-Based Optimization (TLBO) and Particle Swarm Optimization (PSO) algorithms to find the optimum values of the PIDF and Fuzzy-PIDF controllers' gains, respectively. The dual-stage design ensures that the controller maintains functionality even if one stage experiences partial failure, thereby enhancing the reliability of both the controller and the system under control. The tuning process for both stages employs the well-known Integral Time Absolute Error (ITAE) cost function in conjunction with the TLBO and PSO algorithms. The reliability of the proposed controller is rigorously tested, demonstrating its ability to deliver robust performance even when operating partially. A comprehensive comparative analysis with existing techniques in the literature demonstrates the superior performance of the proposed PIDF plus Fuzzy PIDF controller. The results show significant improvements in transient response metrics: overshoot is reduced from 0.1559 pu to 0.0211 pu, undershoot from 0.0954 pu to 0.006 pu, and settling time from 0.7568 seconds to 0.2299 seconds. These advancements underscore the controller's enhanced dynamic stability and precision compared to prior methodologies. Additionally, the robustness of the PIDF + Fuzzy-PIDF controller is evaluated under conditions of system uncertainty and varying load disturbances, with validation conducted in the MATLAB and Simulink environments. The results affirm the controller's superiority, robustness, and reliability, establishing its potential for successful implementation in real-world applications. This study introduces a novel AVR system characterized by exceptional reliability, robustness, and performance, positioning it as a promising solution for practical deployment.

INDEX TERMS Reliable AVR, TLBO algorithm, PSO algorithm, PIDF + fuzzy PIDF, ITAE.

I. INTRODUCTION

A. GENERAL OVERVIEW

The Automatic Voltage Regulator (AVR) is a critical component in electrical engineering, designed to regulate and stabilize the voltage output of electrical generators. Voltage regulation is essential for maintaining the reliability, efficiency, and safety of electrical systems. As modern power systems grow in complexity, the AVR has become indispensable for ensuring stable operation across a variety of applications, from industrial machinery to renewable energy systems [1]. Given its foundational role, it is imperative to first elucidate the principle of operation that underpins the AVR's functionality.

1) PRINCIPLE OF OPERATION

The AVR ensures the stabilization of an alternator's or generator's output voltage by dynamically controlling its

The associate editor coordinating the review of this manuscript and approving it for publication was Jorge Esteban Rodas Benítez.

excitation, thereby maintaining voltage consistency despite fluctuations in load or external disturbances [2]. This process involves three key stages: voltage sensing, where the AVR continuously monitors the system's output voltage; error detection, in which deviations from a predefined reference voltage are identified; and control action, whereby the AVR modulates the excitation current supplied to the generator's field windings to restore the output voltage to the specified target. This integrated mechanism ensures reliable voltage regulation and optimal system performance [3]. An understanding of the AVR's operating principles further accentuates its essential functions within contemporary power systems.

2) KEY FUNCTIONS OF AVR

The AVR performs several critical functions to enhance the reliability and efficiency of power generation systems. Voltage stability is maintained by ensuring consistent output voltage under fluctuating load conditions [4]. Load sharing is facilitated by balancing voltage levels during parallel operation of multiple generators, thereby promoting system harmony. Additionally, the AVR enhances power quality by mitigating voltage fluctuations, surges, and sags, which contributes to improved overall system performance [5]. It also provides system protection by preventing overvoltage and undervoltage conditions that could potentially damage electrical equipment. Lastly, the AVR improves energy efficiency by optimizing generator performance, minimizing power losses, and enhancing fuel utilization [6]. In light of these pivotal functions, the broader significance of the AVR across various critical sectors becomes readily apparent.

3) IMPORTANCE OF AVR

The AVR plays a pivotal role in ensuring the reliability and efficiency of power systems across diverse applications. It guarantees a reliable power supply in critical sectors such as hospitals, data centers, and industrial facilities, where uninterrupted operations are imperative. By maintaining voltage stability, the AVR contributes to an enhanced lifespan of electrical equipment, reducing wear and tear, minimizing maintenance costs, and prolonging the operational durability of components. Furthermore, the AVR is instrumental in facilitating the integration of renewable energy sources, such as solar and wind power, by addressing the voltage stability challenges posed by their intermittent nature. Additionally, the AVR contributes to grid stability by maintaining voltage levels within prescribed limits, thereby ensuring compliance with regulatory grid codes and supporting the seamless operation of power distribution networks [7]. Parallel to its widespread importance, the diverse range of AVR applications underscores its versatility and necessity in modern energy infrastructures.

4) APPLICATIONS OF AVR

The AVR finds extensive application across a variety of sectors, underscoring its significance in modern power systems. In power generation, AVRs are integral to synchronous generators, where they regulate output voltage to align with grid specifications and ensure seamless integration into the power network. Within the realm of industrial automation, AVRs are employed in manufacturing facilities to maintain voltage stability, thereby safeguarding the operation of sensitive and precision-driven equipment. In the domain of consumer electronics, AVRs are embedded in uninterruptible power supply (UPS) systems to provide a consistent and reliable power supply for electronic devices, preventing disruptions or damage caused by voltage fluctuations. Moreover, in renewable energy systems, AVRs are incorporated into inverters and grid-tied configurations to effectively manage the inherent voltage variability of renewable sources such as solar and wind, thereby facilitating their stable integration into the energy grid [8]. Despite these extensive applications, several persistent challenges must be addressed to advance AVR design and operational performance further.

5) CHALLENGES IN AVR DESIGN

The operation of AVRs in modern power systems is confronted with several critical challenges. Dynamic load conditions, characterized by rapidly fluctuating power demands, necessitate the implementation of advanced and adaptive control strategies to preserve system stability [9]. Additionally, harmonic distortions introduced by nonlinear loads pose significant challenges, as they can degrade the performance and precision of AVRs. The integration with smart grids further emphasizes the need for AVRs equipped with real-time communication capabilities and adaptive control mechanisms to meet the demands of intelligent, interconnected power networks [10]. Moreover, achieving an optimal balance between cost and efficiency presents a persistent challenge, as the development of highly sophisticated AVRs must reconcile economic constraints with enhanced functionality and operational efficiency [11].

The AVR is a cornerstone of modern electrical systems, ensuring voltage stability and system reliability across diverse applications. Its role in enhancing power quality, protecting equipment, and supporting renewable energy systems underscores its importance in both academic research and industrial practices. Continued advancements in AVR technology, driven by innovations in control algorithms and integration with smart grids, will further cement its significance in the evolving landscape of power engineering [12]. These design challenges have catalyzed extensive research efforts focused on the development and optimization of advanced control methodologies, as discussed in the following literature review.

B. LITERATURE REVIEW

Despite the advent of modern control theories and techniques, the proportional-integral-derivative (PID) controller remains the predominant choice for AVR systems. The control mechanism of a PID controller is defined by three key parameters: proportional gain (Kp), integral gain (Ki), and derivative gain (Kd). These parameters form the basis of the PID control law, which integrates three distinct control strategies to achieve system stability and performance [13].

Although the classical PID controller is well-established for its effectiveness in AVR systems, its inherent limitations have spurred significant research into advanced control variants. To overcome these constraints, scholars have proposed numerous sophisticated adaptations in the literature, aiming to enhance dynamic adaptability, ensure robust performance, and optimize overall control efficacy.

These sophisticated configurations are designed to mitigate the inherent limitations of the conventional PID framework, thereby providing more resilient and adaptive control solutions that align with the dynamic demands of contemporary power systems. Among these advancements are the PID controller with acceleration gain (PIDA), and Tilt-Integral-Derivative (TID) controller. Furthermore, recent advancements have explored extending the conventional PID framework through the incorporation of fractional calculus into the integral and derivative components. This extension gives rise to the Fractional-Order PID (FOPID) controller, which expands the control law to five parameters, offering enhanced adaptability and precision. The inclusion of fractional calculus in the FOPID controller introduces fractional-order integration and differentiation, enabling greater flexibility in addressing complex system dynamics [14]. Empirical studies have substantiated that the FOPID, TID and PIDA controllers are likely to surpass the performance of the conventional PID controller in various operational scenarios. However, the implementation of fractional calculus is inherently more intricate than traditional integer-order derivatives and integrals. To harness the full potential of the FOPID controller, careful tuning of all five parameters is imperative [15].

Notably, the increased parametric complexity of these advanced controllers—particularly the FOPID's five-dimensional tuning space—exacerbates the limitations of classical tuning methodologies like Ziegler-Nichols (ZN) or Cohen-Coon. These conventional strategies, reliant on linearized assumptions and empirical rules, prove inadequate for optimising high-dimensional, nonlinear control systems, often resulting in suboptimal gains, oscillatory responses, or compromised stability. This challenge underscores the critical role of heuristic optimization algorithms—such as Genetic Algorithms (GA), Particle Swarm Optimization (PSO), and Simulated Annealing (SA)—in bridging the gap between theoretical controller design and practical implementation. By systematically exploring the expanded solution space of advanced PID variants, metaheuristic techniques circumvent the rigidity of classical tuning, enabling precise calibration of parameters to meet conflicting objectives like transient damping, steady-state accuracy, and computational efficiency. [16]. This paper provides a comprehensive discussion of these heuristic approaches and their application in designing optimal controllers for AVR systems based on PID and its variants.

Importantly, before discussing the most common control technologies reported in the literature for AVR applications, it is worth highlighting that advanced control strategies, such as adaptive control and sliding mode control (SMC), have demonstrated significant potential for enhancing the robustness and adaptability of AVR systems [17]. Adaptive control, in particular, dynamically adjusts controller parameters in real-time to accommodate variations in system dynamics, making it especially effective in environments characterized by high uncertainty or fluctuating load conditions. This approach has been successfully deployed in complex systems, including aerospace applications, where performance demands are stringent. Despite its advantages, adaptive control is often associated with high design complexity and the need for precise real-time parameter tuning, which can impede its practical implementation in AVR systems due to computational and operational challenges [18]. Similarly, sliding mode control (SMC) is highly regarded for its resilience to matched uncertainties and its capacity to ensure system trajectories remain confined within a predetermined sliding manifold, effectively mitigating the impact of disturbances. SMC has been extensively validated in applications such as power electronics and voltage regulation, where its precision and reliability are critical [19]. However, its practical adoption is frequently constrained by the chattering phenomenon, which is a high-frequency oscillatory behavior caused by the discontinuous nature of the control signal. Chattering not only degrades system performance but also poses risks of mechanical and electrical wear, particularly in sensitive applications. Addressing these challenges is essential for unlocking the full potential of adaptive control and SMC in AVR systems, paving the way for their broader adoption in modern power regulation [20].

As previously emphasized, the PID controller persists as the predominant feedback control mechanism in contemporary engineering systems, constituting over 90% of all industrial control loops [21]. Within AVR applications, scholarly research highlights that the majority of recently developed control strategies remain fundamentally grounded in the PID framework. These methodologies are deployed either as standalone controllers, enhanced configurations (e.g., cascaded or gain-scheduled structures), or hybrid architectures integrating complementary control paradigms, such as adaptive or intelligent systems. Recent advancements have focused extensively on computational optimization techniques to refine PID parameter tuning in AVR systems. A diverse array of metaheuristic algorithms has been proposed, including Biogeography-Based Optimisation

(BBO) [22], Particle Swarm Optimization (PSO) [23], an Enhanced PSO (EPSO) [24], Grasshopper Optimisation Algorithm (GOA) [25], Local Unimodal Sampling Algorithm (LUSA) [26], Pattern Search Algorithm (PSA) [27], Artificial Bee Colony (ABC) [28], Sine-Cosine Algorithm (SCA) [29], Many Optimizing Liaisons (MOL) [30], Improved Whale Optimization Algorithm (IWOA) [31], Tree Seed Algorithm (TSA) [32], Symbiotic Organisms Search Algorithm (SOSA) [33], Naked Mole Rat Algorithm (NMRA) [34], World Cup Optimisation Algorithm (WCOA) [35], and Water Wave Optimisation Algorithm (WWOA) [36].

To leverage the advantages of alternative PID controller variants in AVR applications, the PIDA controller optimized via the Whale Optimization Algorithm (WOA) is proposed and empirically validated in [37]. This method has showcased enhanced performance compared to the traditional PID controller optimized with the same algorithm. Similarly, various optimization techniques, including Harmony Search (HS), were utilized in [38] to fine-tune both PID and PIDA controllers for AVR applications. These optimized designs demonstrated reliable and robust performance under diverse operating conditions.

Similarly, an enhanced variant of the classical PID controller—the PID controller with filtered derivative action (PIDF), characterized by four independently tunable parameters—was proposed by [39] for AVR applications. This configuration leveraged the Symbiotic Organism Search Algorithm (SOSA) to optimize its parameters, yielding enhanced precision and superior operational performance. Building on this progression, [40] introduced a novel PID-based architecture for AVR systems by incorporating dual derivative actions, culminating in a PID plus second-order derivative (PIDD^2) controller. The parameters of this $PIDD^2$ structure were systematically optimized via the Particle Swarm Optimization (PSO) algorithm, with comparative analyses revealing its improved transient response characteristics relative to conventional PID implementations.

The widely studied fractional-order PID (FOPID) controller, an advanced evolution of traditional PID control, has also been successfully applied to AVR systems. For instance, [41], demonstrated an FOPID controller optimized through the Dumbo Octopus Algorithm (DOA), achieving robust performance in voltage regulation. Further innovations include the Chaotic Yellow Saddle Goatfish Algorithm (C-YSGA), proposed in [42], which was shown to surpass existing methodologies in tuning FOPID parameters for AVR applications, delivering exceptional dynamic performance. Additionally, [43] investigated an FOPID controller calibrated using a refined variant of the Marine Predators Algorithm (MPA), underscoring its efficacy in stabilizing AVR systems under diverse operational conditions.

Other more advanced AVR systems based on PID and FOPID theories have been proposed in the literature in order to achieve a further superior performance. For instance, [44] introduces the Quadratic Wavelet-Enhanced Gradient-Based Optimization (QWGBO) algorithm, enhancing AVR robustness and efficiency by refining gradient-based methods with quadratic interpolation and wavelet mutation strategies. The QWGBO is coupled with a cascaded Real PID with second-order derivative $RPIDD^2$ and FOPI controller, demonstrating superior optimization and transient response performance.

Further innovations include the work of [45], which proposes the fractional-order integral-derivative plus second-order derivative controller with low-pass filters ($I^{\lambda}DND^2N^2-T$). This hybrid configuration is optimized using Equilibrium Optimisation (EO), multiverse optimisation (MVO), and PSO algorithms. It excels in robustness against system parameter variations and disturbances, including frequency deviation, load changes, and short circuits. Reference [11] develops a Modified Hybrid Fractional-Order (MHFO) AVR equipped with a fractional-order tilt integral and proportional derivative with a filter plus a second-order derivative with a filter FOTI- $PDND^2N^2$ controller, optimized with the Growth Optimizer (GO). This approach offers extensive tunable parameters, enhancing stability, robustness, and dynamic response over existing controllers. A novel $PIDND^2N^2$ controller optimized with the balanced Arithmetic Optimization Algorithm (b-AOA), integrating pattern search and elite opposition-based learning is introduced in [46]. This method achieves minimal rise and settling times, robust frequency response, and superior stability compared to state-of-the-art techniques.

Furthermore, a novel tilt-fractional order integral-derivative with a second order derivative and low-pass filters controller, referred to as $TI^{\lambda}DND^2N^2$ controller, optimized via the Equilibrium Optimizer (EO) algorithm is proposed in [47] to improve transient and frequency response. It surpasses conventional and hybrid controllers in control performance, robustness, and stability under system perturbations. Reference [48] presents low-order approximation (LOA) of FOPID for an AVR based on the Modified Artificial Bee Colony (MABC), reducing complexity in fractional-order PID implementation while optimizing performance using an improved variant of the ABC algorithm. Comparative analyses show its superior transient and robustness characteristics over advanced optimization techniques. A novel 3-degrees-of-freedom-PID-Acceleration (3)-DOF-PIDA) controller combined with a disturbance observer and Salp Swarm Optimization Algorithm (SSOA) is introduced in [5]. This approach enhances AVR performance by continuously adapting parameters and compensating for external disturbances, ensuring superior voltage regulation under fluctuating conditions. These innovations collectively advance AVR technology, achieving remarkable improvements in precision, stability, robustness, and adaptability for modern power systems. Table 1 provides a detailed classification of various control methodologies, tuned by different optimization algorithms that have been reported in the literature for AVR applications.

Recent advances in fuzzy control have significantly expanded the toolkit for nonlinear systems, with notable developments including Interval Type-2 Fuzzy Logic Controllers (IT2-FLCs) and Adaptive Neuro-Fuzzy PID (ANF-PID) systems. For instance, [49] proposes an Optimal Hybrid Interval Type-2 Fuzzy PID+I (OH-IT2FPID+I) controller based PSO algorithm for multi-degree-of-freedom oil well drill-string systems. Meanwhile, [50] introduces a Hybrid Interval Type-2 Fractional Order Fuzzy PID (IT2FO-FPID) controller, which leverages a fractional-order integro-differentiator to combine the advantages of IT2-FLCs and FOPID controllers. The study evaluates various IT2FO-FPID structures on different fractional-order processes, followed by robustness analysis. Additionally, a Fast Intelligent Cascade Control Scheme (CFF-NFPID), integrating hybrid adaptive neuro-fuzzy PID with feedforward terms, has been proposed in [51] for drill-string systems. While these methods show promise for highly nonlinear systems, they may face challenges that may limit their suitability for real-time AVR applications requiring rapid response and minimal hardware complexity. However, with careful design and optimization, these strategies can be adapted for AVR systems. This further motivates the proposed hybrid control approach, which retains the simplicity of Type-1 fuzzy logic while enhancing reliability through a parallel structure tailored for voltage regulation.

C. MOTIVATION AND CONTRIBUATIONS

In AVR systems, achieving an optimal balance between fast response and stability is a longstanding objective among researchers and engineers. A rapid response with slight overshoot enables quick voltage stabilization, which is crucial in dynamic environments characterized by frequent and abrupt load changes. This ensures the system can swiftly restore voltage levels after disturbances, minimizing downtime and maintaining operational continuity. However, such rapid responses may temporarily exceed safe voltage thresholds, potentially causing damage to sensitive electronic equipment. Conversely, a slower response with no overshoot ensures voltage remains within safe limits, protecting equipment but risking temporary undervoltage or overvoltage during load transitions, which can compromise performance and reliability in critical applications.

Despite various techniques addressing voltage stabilization effectively, challenges such as robustness, design complexity, ease of implementation, and sensitivity to nonlinearities persist. Many existing approaches, including traditional PID controllers, adaptive control and SMC still face limitations. While PID controllers are simple and cost-effective, they often fail to meet the demands of modern AVR systems. Adaptive control and SMC offer robustness but suffer from implementation complexity and computational overhead. These shortcomings highlight the need for innovative control strategies that deliver enhanced reliability, robustness, and simplicity for AVR systems in dynamic and uncertain environments.

TABLE 1. List of controllers and optimization techniques for AVR.

Ref	Year	Controller	Optimization tool	No of tuned Parameters
22	2016	PID	BBO	3
23	2004	PID	GA & PSO	3
24	2025	PID	EPSO	3
25	2018	PID	GOA	3
26	2014	PID	LUSA	3
27	2012	PID	PSA	3
28	2011	PID	ABC	3
29	2019	PID	SCA	3
30	2012	PID	MOL	3
31	2022	PID	IWOA	3
32	2020	PID	TSA	3
33	2018	PID	SOSA	3
34	2023	PID	NMRA	3
35	2016	PID	WCOA	3
36	2019	PID	WWOA	3
37	2019	PIDA	WOA	4
38	2018	PIDA	HS	4
39	2022	PIDF	SOSA	4
40	2015	$PIDD^2$	PSO	4
41	2024	FOPID	DOA	5
42	2020	FOPID	C-YSGA	5
43	2023	FOPID	MPA	5
44	2024	$RPIDD^2 - FOPI$	QWGBO	9
45	2024	$I^{\lambda}DND^2N^2$-T	MVO & PSO	8
11	2024	FOTI-$PDND^2N^2$	GO	9
47	2023	$PIDND^2N^2$	b-AOA	6
48	2023	$TI^{\lambda}DND^2N^2$	EO	8
49	2022	LOA-FOPID	MABC	5
5	2024	3-DOF-PIDA	SSOA	10

This paper introduces a novel hybrid AVR controller that integrates the simplicity of PID control with the adaptability of fuzzy logic to form a reliable and effective AVR controller. The key contributions of this study are as follows:

1. Innovative Controller Design: A unique AVR configuration tuned in two stages is proposed, combining a PID-with-filtered derivative action (PIDF) controller with additional components, including an FLC with PIDF and FOPD controllers. This hierarchical design enhances system stability and reliability, ensuring continued control functionality even if one part of the structure fails.
2. Optimization Framework: The primary PIDF controller is optimized using the well-known Teaching-Learning-Based Optimization (TLBO) algorithm, while the additional parts are fine-tuned using the widely used and successfully implemented PSO algorithm. Both algorithms have demonstrated superior performance across a wide range of applications. Moreover, they are known for their simplicity and implementation efficiency.

3. Comprehensive Comparative Analysis: A detailed comparison is conducted between the proposed controller and existing methods reported in the literature, demonstrating its superior performance.
4. Robustness Assessment: The proposed controller undergoes rigorous testing against parametric uncertainties and various load disturbances. Results demonstrate its resilience and reliability in maintaining voltage stability under challenging conditions.

This study advances the field of AVR control by addressing key limitations and delivering a robust, reliable, and innovative solution for modern power systems.

D. PAPER STRUCTURE

This research paper is structured as follows: Section Two outlines the mathematical modeling of the AVR system and evaluates its step response in the absence of a controller. Section Three delves into the structure of the proposed controller, offering a detailed explanation of the optimization techniques employed and the formulation of the objective function. Section Four presents and analyzes the results obtained from the study. Section Five assesses the robustness of the AVR system in different scenarios when integrated with the designed controller. Lastly, Section Six concludes the study with a summary of key findings and suggests potential avenues for future research.

II. AVR MODEL

Figure 1 provides a schematic representation of the mechanism underlying the AVR system. The AVR system comprises four principal components: the amplifier, exciter, sensor, and generator. These components are interconnected in a feedback loop, with control strategies employed to correct deviations in the generator's terminal voltage. This regulation ensures stable voltage levels, which are crucial for maintaining the overall stability of the power system.

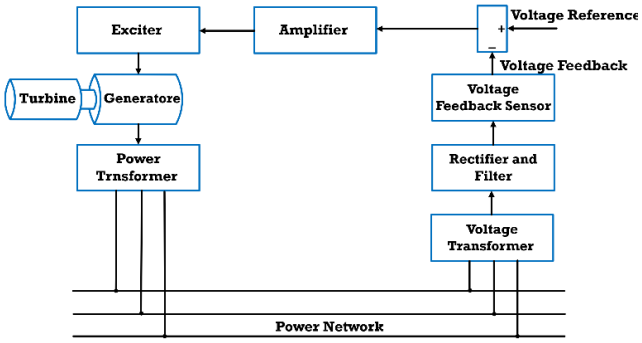

FIGURE 1. AVR schematic diagram.

Figure 2 presents the typical block diagram of the AVR system, where each component is represented by a transfer function that links its input to its output. The key parameters of the AVR system include gains *Ka*, *Ke*, *Kg*, and *Ks*, as well as time constants *Ta*, *Te*, *Tg*, and *Ts*, corresponding to the amplifier, exciter, generator, and sensor, respectively. These parameters, modelled as linear devices, are drawn from previous studies and are presented in Table 2.

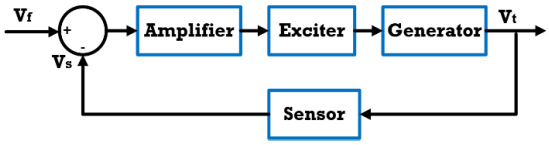

FIGURE 2. AVR block diagram.

TABLE 2. The AVR system parameters.

AVR component	Transfer Function	Implemented Value
Generator	$\frac{K_g}{1+s\tau_g}$	K_g=1, τ_g= 1
Excitor	$\frac{K_e}{1+s\tau_e}$	K_e=1, τ_e= 0.4
Sensor	$\frac{K_s}{1+s\tau_s}$	K_s=1, τ_s= 0.01
Amplifier	$\frac{K_a}{1+s\tau_a}$	K_g=10, τ_g= 0.1

The closed-loop transfer function of the AVR model, based on the parameters specified in Table 2, is shown in Equation 1. The system's step response is illustrated in Figure 3, with its key performance characteristics summarized in Table 3.

$$TF_{AVR} = \frac{0.1\,s + 10}{0.0004\,s^4 + 0.045\,s^3 + 0.555\,s^2 + 1.51\,s + 11} \quad (1)$$

The root locus plot in Figure 4 reveals the presence of one zero at -100, two real poles at $-99.9712 + 0$ i & $-12.4892 + 0$ i and two complex poles at $-0.5198 + 4.6642$i & $-0.5198 - 4.6642$i. This analysis highlights several performance limitations, including significant steady-state error, prolonged settling times, and excessive overshoot.

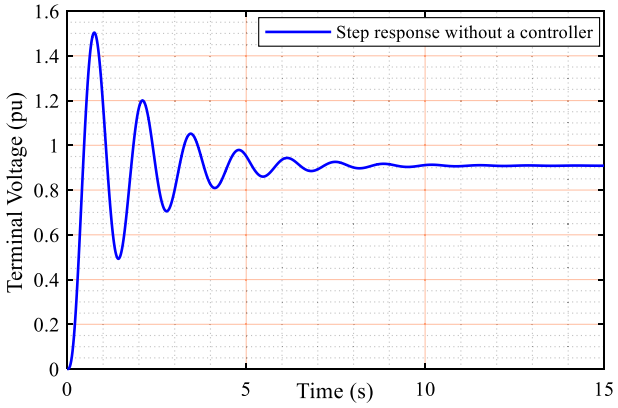

FIGURE 3. Step response without a controller.

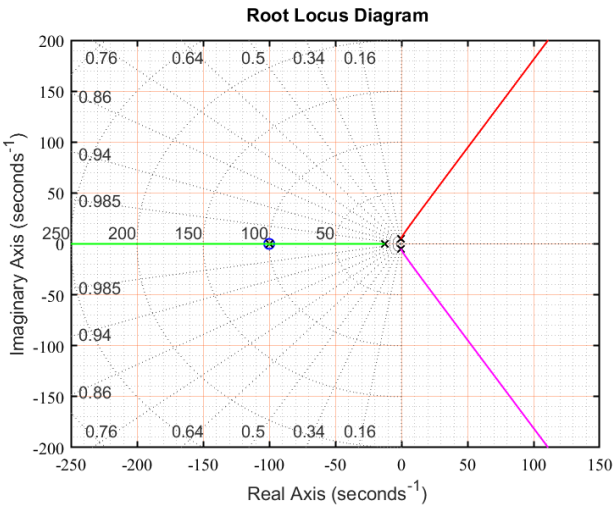

FIGURE 4. The root locus of the AVR uncontrolled model.

TABLE 3. The characteristics of the uncontrolled AVR model.

Characteristics	Value
Peak Overshoot	1.5066 pu
Peak Time	0.7522 s
Settling Time	6.9865 s
Rise Time	0.2607 s

The empirical findings underscore the necessity of improving the steady-state accuracy and transient response characteristics of the AVR system. The primary objective of the AVR system is to ensure a stable voltage output despite disturbances or fluctuations in load. However, the step response analysis of the uncontrolled AVR system reveals significant deficiencies. These include its failure to converge to the desired output, extended time to reach a steady state after a disturbance, and overshooting the desired voltage level.

To address these challenges, various control strategies have been developed and implemented for the AVR system. These strategies are elaborated upon in the subsequent sections.

III. PROPOSED CONTROLLER AND OPTIMISATION TOOLS

A. THE ENHANCED PIDF TUNED IN TWO STAGES

This design presented in Figure 5 aims to achieve not only exceptional control performance but also a high degree of reliability, thereby fulfilling the requirements for maintaining voltage stability. The proposed hierarchical control design operates in two stages that function concurrently, with each stage being individually optimized.

To ensure the effectiveness of the primary controller, a PID with Filter (PIDF), it is initially tuned independently using the Teaching-Learning-Based Optimization (TLBO) algorithm. Subsequently, to further enhance the PIDF's performance, an additional controller is incorporated. The control actions of both controllers are combined to generate the final control signal. The second controller is tuned using the PSO Algorithm, with the optimization process accounting for the optimal gains of the PIDF obtained during the first stage.

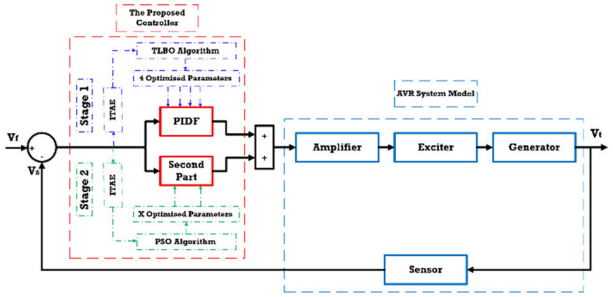

FIGURE 5. The proposed control configuration.

It is important to note that various controllers are evaluated as potential enhancements to the primary PIDF, with detailed discussions provided in the following subsections. This hierarchical control design significantly improves system stability and reliability, ensuring continued control functionality even in the event of partial system failure.

1) THE PRIMARY PIDF

The PIDF (Proportional-Integral-Derivative with Filter) controller represents an enhanced version of the conventional PID controller, offering superior performance in specific applications by addressing the inherent limitations of standard PID control. One of the primary advantages of PIDF is its ability to mitigate noise sensitivity in the derivative term, which, in traditional PID controllers, can lead to erratic control actions and instability due to high-frequency disturbances. By incorporating a low-pass filter on the derivative component, PIDF effectively smooths out noise, resulting in a more robust and stable control response. Furthermore, this reduction in noise amplification enhances system stability, allowing for improved performance, particularly in environments with significant external disturbances. Real-world systems are often subject to noise and unpredictable variations, which can degrade the effectiveness of a standard PID controller. The filtered derivative term in PIDF ensures that the controller responds more accurately to actual system dynamics rather than reacting to noise, thereby facilitating smoother and more precise control. Additionally, PIDF introduces a filter time constant as an extra tuning parameter, offering greater flexibility in optimizing system response, particularly in scenarios where traditional PID struggles due to noise or high-frequency dynamics. Another key advantage of PIDF is its ability to reduce overshoot and oscillations, leading to improved transient performance, shorter settling times, and enhanced overall system stability. Consequently, PIDF is a more effective choice in applications where noise robustness, stability, and precise tuning are critical. The transfer function of the PIDF controller is presented in Equation 2 where K_p, K_i, K_d and K_F are the proportional,

integral, derivative and filter gains, respectively.

$$\mathrm{PIDF_c}\,(S) = K_p + \frac{K_i}{S} + \frac{K_d K_F}{1 + K_F \frac{1}{S}} \tag{2}$$

This controller is tuned via the well-known TLBO algorithm in order to determine the optimal values of its parameters. The tuning process is well explained in the following subsections.

2) PIDF PLUS FUZZY LOGIC CONTROL WITH PIDF

As previously mentioned, the main objective is to enhance the primary PIDF controller by integrating it with various control strategies to identify the optimal configuration that effectively functions as an AVR controller. It is well-established that Fuzzy Logic Control (FLC) represents an intelligent control methodology capable of operating robustly across diverse environments and under varying conditions for a wide range of applications, while consistently delivering superior control performance. Consequently, an FLC-based approach is proposed to augment the primary PIDF controller, thereby improving the overall system performance. This structure is presented in Figure 6.

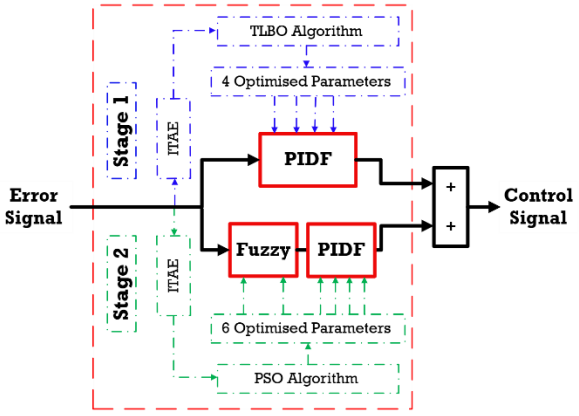

FIGURE 6. The PIDF plus Fuzzy PIDF structure for AVR.

Upon determining the optimal gains of the PIDF controller through the TLBO algorithm, an FLC connected with PIDF (Fuzzy PIDF) is integrated into the control structure. The Fuzzy Logic Controller (FLC) is systematically structured with two principal input variables: the error signal and its time derivative. These inputs are normalized through input scaling factors, designated as K_1&K_2, respectively. The controller generates a singular output, which is integrated with a PIDF controller architecture. Specifically, the resultant signal from the Fuzzy PIDF controller is amalgamated with the control output of the primary PIDF controller to synthesize the composite control signal. This hybrid configuration leverages the adaptive capabilities of fuzzy logic alongside the deterministic dynamics of the PIDF framework to enhance overall system performance.

To optimize system efficiency while maintaining structural simplicity, the FLC implements a quintuple trapezoidal and triangular membership function configuration for the input and output linguistic variables. As illustrated in Figure 7, these membership functions are strategically designated as Negative Big (NB), Negative Small (NS), Zero (Z), Positive Small (PS), and Positive Big (PB). The inference mechanism operates through a comprehensive rule base (Table 4), comprising 25 fuzzy conditional statements.

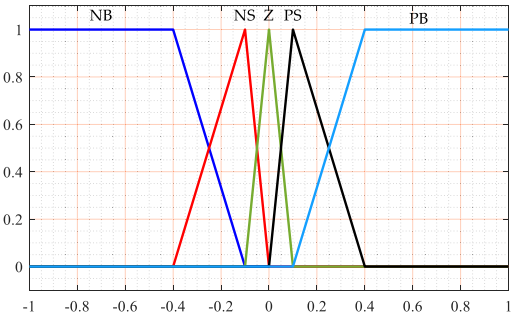

FIGURE 7. The membership functions of the FLC.

TABLE 4. The rule base of the fuzzy controller.

Error	Change of Error				
	NB	NS	Z	PS	PB
NB	NB	NB	NB	NS	Z
NS	NB	NB	NS	Z	PS
Z	NB	NS	Z	BS	PB
PS	NS	Z	PS	PB	PB
PB	Z	PS	PB	PB	PB

The Mamdani inference methodology is employed to execute the fuzzification process, enabling the systematic conversion of crisp input data into fuzzy linguistic variables. For the defuzzification phase, the Centroid technique is implemented to derive a precise, real-valued control signal by calculating the geometric center of the aggregated fuzzy output set. Furthermore, the gain parameters K_1, K_2K_p, K_i, K_d and K_F are optimized using the PSO algorithm, taking into account the PIDF controller with its previously determined optimal gains from the initial stage.

3) PIDF PLUS FRACTIONAL ORDER PD

In this structure, the main PIDF is enhanced by a Fractional Order Proportional-Derivative (FOPD) controller, as shown in Figure 8. The transfer function of the proposed controller is expressed in Equation 3, μ is the order of differentiator, K_{p1} is the proportional gain and K_{d1} is the derivative gain of the FOPD controller.

$$\mathrm{PIDF + FOPD_c}\,(S) = K_p + \frac{K_i}{S} + \frac{K_d K_F}{1+K_F \frac{1}{S}} + K_{p1} + K_{d1} S^{\mu} \tag{3}$$

B. TLBO ALGORITHM

The primary PIDF controller is meticulously tuned using the widely acclaimed Teaching-Learning-Based Optimization (TLBO) algorithm, a robust population-based heuristic

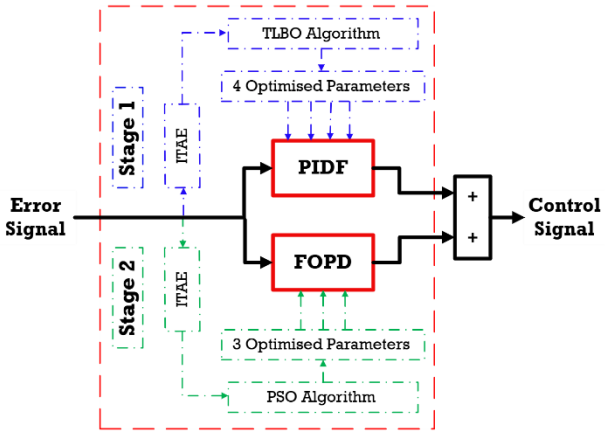

FIGURE 8. The PIDF plus FOPD structure for AVR.

optimization technique. Inspired by the dynamics of teaching and learning processes in a classroom, the TLBO algorithm effectively simulates the interaction between a teacher and students to achieve optimal parameter tuning. This approach ensures superior performance and adaptability of the controller in dynamic environments. The algorithm operates in two main phases: the Teaching Phase and the Learning Phase.

1) TEACHING PHASE

In this phase, the algorithm mimics the process of a teacher imparting knowledge to students. The teacher, representing the best solution in the population, strives to improve the average performance of the class (population). The steps are as follows:

- ➢ Identify the Teacher: The best solution in the population is selected as the teacher.
- ➢ Calculate the Mean: The mean performance of the class (average of all solutions) is calculated.
- ➢ Update Solutions: The teacher attempts to improve the mean performance of the class by moving the solutions toward the teacher's level. The difference between the current mean and the new mean (influenced by the teacher) is calculated, and the solutions are updated accordingly.

2) LEARNING PHASE

In this phase, students enhance their knowledge through mutual interaction and collaboration. The steps are as follows:

- ➢ Random Pairing: Two students (solutions) are randomly selected from the population.
- ➢ Knowledge Sharing: The students compare their performance and update their knowledge based on the better-performing student. If one student performs better, the other student learns from them; otherwise, the learning occurs in the opposite direction.
- ➢ Update Solutions: The solutions are updated based on this interaction, ensuring continuous improvement in the population.

A comprehensive explanation of the TLBO algorithm, including its underlying mechanism, flowchart, mathematical formulations, and step-by-step implementation, can be found in the referenced literature [17], [52]. These sources provide detailed insights into the algorithm's operation, its phases (teaching and learning), and its application in optimising complex systems.

To ensure a sensible computational time for parameter tuning, the algorithm's population size and the number of iterations were both set to 50 in this study.

C. PSO ALGORITHM

Particle Swarm Optimization (PSO) is a metaheuristic algorithm inspired by the collective dynamics of biological systems, such as avian flocks or fish schools. The algorithm initializes a swarm of particles, each representing a candidate solution, which traverse the multidimensional search space. Particle trajectories are iteratively updated through a synthesis of individual historical performance (*pbest*) and the swarm's global best solution (*gbest*). Specifically, each particle adjusts its velocity and position using weighted contributions from its own optimal experience and the swarm's collective intelligence. This dual mechanism balances exploration (diversifying search efforts) and exploitation (refining known solutions), enabling PSO to efficiently navigate complex, non-convex optimization landscapes. A comprehensive discussion of the algorithm's theoretical foundations and implementation is presented in [53] and [54].

The PSO parameters employed in this study are enumerated in Table 5. Maximum iterations define the termination criterion, limiting computational expense is set to 50 in this study. Below, we define their roles in modulating algorithmic behavior:

- ➢ Number of Particles (50): Determines swarm size, directly influencing solution diversity and computational load.
- ➢ Inertia weight range (Wmax = 1.2, Wmin = 0.2): Governs momentum preservation. Higher initial weights (Wmax) prioritize global exploration, while linearly decreasing weights (to Wmin) enhance local exploitation over iterations.
- ➢ Cognitive and social coefficients (C1 = 1.2, C2 = 1.2): Control particle attraction to pbest (self-learning) and gbest (social learning), respectively.
- ➢ Velocity constraints (Vmax = 0.2(ub – lb), Vmin = −Vmax): Confine particle velocities to 20% of the search space range (ub = upper bound, lb = lower bound), preventing oscillatory divergence while maintaining search efficacy.

These parameters collectively calibrate the exploration-exploitation equilibrium, critically affecting convergence speed and solution precision.

D. COST FUNCTION

In control theory, achieving a balance between fast response and system stability is a critical yet challenging objective.

TABLE 5. The PSO parameters.

No Particles	Wmax	Wmin	C1	C2	Vmax	Vmin
50	1.2	0.2	1.2	1.2	(ub-lb)*0.2	-Vmax

These two performance metrics often conflict, as optimizing one can adversely affect the other. Effective control design, therefore, requires a careful equilibrium between rapid response and robust stability. This is accomplished through the selection of an appropriate controller structure and the minimization of a well-defined objective function, often facilitated by advanced optimization techniques.

Among the commonly used performance criteria in control system design, the Integral of Time-Weighted Absolute Error (ITAE), Integral of Squared Error (ISE), Integral of Time-Weighted Squared Error (ITSE), and Integral of Absolute Error (IAE) are widely recognized. The ISE and ITAE criteria are particularly prominent in the literature due to their superior performance compared to IAE and ITSE.

The ISE criterion evaluates the integral of the squared error over time, emphasizing larger errors due to the quadratic nature of the function. While this approach ensures rapid elimination of significant errors, it may permit smaller errors to persist over time, often resulting in systems with fast response times but accompanied by low-amplitude oscillations. In contrast, the ITAE criterion integrates the absolute error weighted by time, prioritizing errors that persist over longer durations. This characteristic typically leads to systems with faster settling times and improved transient performance compared to those tuned using ISE.

In this study, the parameters of the proposed controller for AVR applications are optimized in two stages using the TLBO and PSO algorithms. The optimization process minimizes the ITAE objective function, mathematically expressed as:

$$\text{Objective function} = \text{ITAE} = \int_0^t |e| \, .t.dt \tag{4}$$

IV. RESULTS AND DISCUSSION

This research was conducted using MATLAB 2024a, where the TLBO and PSO algorithms were implemented in.m files, while the AVR system and the proposed controller were modelled and simulated in the MATLAB Simulink environment. A step response with an amplitude of 1 per unit (pu) was set as the reference input to evaluate the system's performance. To demonstrate the superiority of the proposed control technique, the obtained results were compared with other methodologies reported in the literature, specifically PID controllers-based GA [23], GOA [25], IWOA [31], and TSA [32]. The PID gains utilized in these comparative studies are summarized in Table 6.

The tuning process was carried out in two stages. In the first stage, the optimal parameters of the primary PIDF controller were determined using the TLBO algorithm. The convergence curve for this optimization process is illustrated in Figure 9, and the optimal values of the PIDF controller are presented in Table 7. In the second stage, the parameters of the Fuzzy PIDF and FOPD controllers were independently optimized using the PSO algorithm. This optimization was performed while considering the optimal values of the PIDF controller obtained in the first stage. The convergence curve for the PSO algorithm, which tuned the Fuzzy PIDF and FOPD controllers, is also presented in Figure 9, and the optimal values for these controllers are detailed in Table 7.

TABLE 6. PID optimal parameters from the literature.

Controller	Parameters		
	K_P	K_I	K_D
PID-TSA	1.1281	0.9567	0.5671
PID-IWOA	0.8167	0.6898	0.2799
PID-GOA	1.3825	1.4608	0.5462
PID-GA	0.8851	0.7984	0.3158

TABLE 7. The optimal parameters of the proposed controller.

Controller		Parameters					
First stage	PIDF	K_p		K_i	K_d		K_f
		0.699		0.4914	0.2153		400
Second stage	FOPD	K_p		K_d		μ	
		0.001		0.008		01.7473	
	Fuzzy PIDF	K_1	K_2	K_p	K_i	K_d	K_f
		0.99	0.041	2	1.52	2	397.78

The two-stage optimization approach ensures a systematic and robust tuning process, where the TLBO algorithm first refines the PIDF controller, and the PSO algorithm subsequently optimizes the advanced control components. This methodology not only enhances the overall performance of the AVR system but also demonstrates the effectiveness of the proposed hybrid control strategy in achieving superior dynamic response and stability compared to existing techniques.

The transient and steady-state performance of the AVR system was quantitatively assessed using five key metrics: peak overshoot (POs, in per unit), peak undershoot (PUs, in per unit), settling time (Ts, in seconds), rise time (Tr, in seconds), and the ITAE cost function value. These metrics are systematically presented in Table 8. Figure 10 illustrates the dynamic response characteristics of the AVR system under the proposed hybrid PIDF + Fuzzy PIDF control architecture. For comparative analysis, the system's performance is benchmarked against conventional PID controllers optimized via established tuning algorithms reported in prior literature.

The proposed PIDF + Fuzzy PIDF controller demonstrates superior performance across all metrics, achieving the fastest settling time Ts = 0.2299, rise time Tr = 0.1300s, and the lowest ITAE value (0.01228), along with the second minimal POs (0.0211 pu) and PUs (0.006 pu). This highlights its

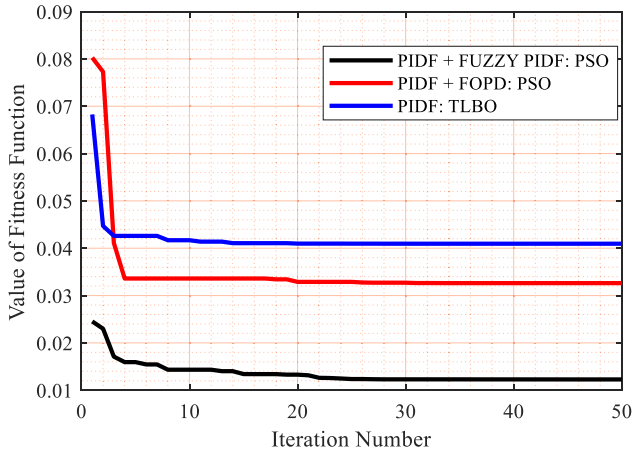

FIGURE 9. The Convergence curves of TLBO and PSO algorithms.

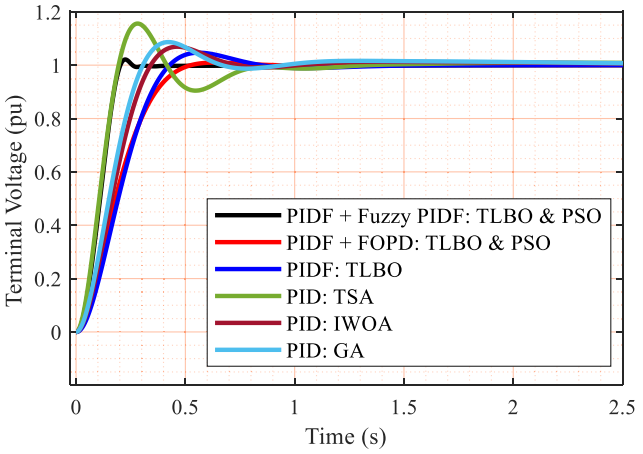

FIGURE 10. The dynamic response of the AVR model based on different control techniques.

exceptional ability to mitigate oscillations, accelerate convergence, and minimize cumulative tracking errors.

By contrast, the PIDF + FOPD controller exhibits marginally higher Ts (0.4654 s) and ITAE (0.03263), though it achieves the lowest POs (0.0096 pu) and PUs (0.001 pu). Traditional optimization-tuned PID controllers, such as PID-GA (ITAE = 0.07652) and PID-TSA (ITAE = 0.08791), show significantly degraded performance, with elevated overshoots (e.g., PID-TSA: POs = 0.1559 pu) and prolonged settling times (PID-TSA: Ts = 0.7568s). Notably, the PIDF-TLBO controller strikes a balance between Ts (0.7312 s) and Tr (0.2762 s), yet its ITAE (0.04095) remains substantially higher than the proposed hybrid architecture.

These results underscore the efficacy of integrating fuzzy logic with PIDF structures to enhance dynamic responsiveness and stability in AVR systems, outperforming both conventional and metaheuristic-optimized PID variants.

TABLE 8. The transient and steady-state performance of several AVR systems.

Controller	POs	PUs	Ts	Tr	ITAE
PIDF+Fuzzy PIDF	0.0211	0.006	0.2299	0.1300	0.01228
PIDF+FOPD	0.0096	0.001	0.4654	0.3079	0.03263
PIDF-TLBO	0.0467	0.011	0.7312	0.2762	0.04095
PID-GA	0.0864	0.013	0.6055	0.2042	0.07652
PID-IWOA	0.06917	0.0088	0.6465	0.2258	0.07078
PID-TSA	0.1559	0.0954	0.7568	0.1311	0.08791

Figures 11–14 present a systematic comparative assessment of dynamic performance metrics for automatic voltage regulator (AVR) control systems employing distinct methodologies, including the novel PIDF + Fuzzy PIDF tuned in two stages.

Figure 11 delineates a comparative evaluation of transient response characteristics, specifically settling time and rise time, across multiple control techniques. Figure 12 quantifies the efficacy of each method through a bar chart analysis

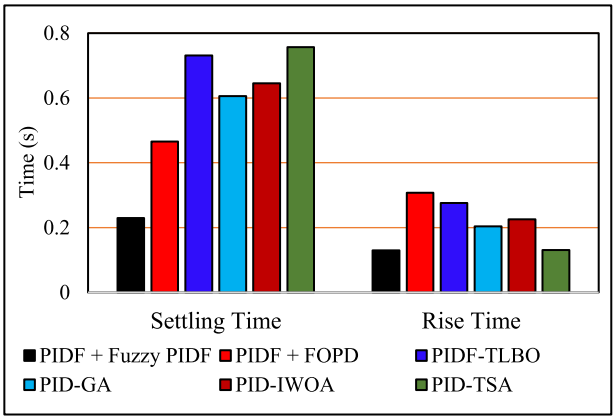

FIGURE 11. The settling time and the rise time of different techniques.

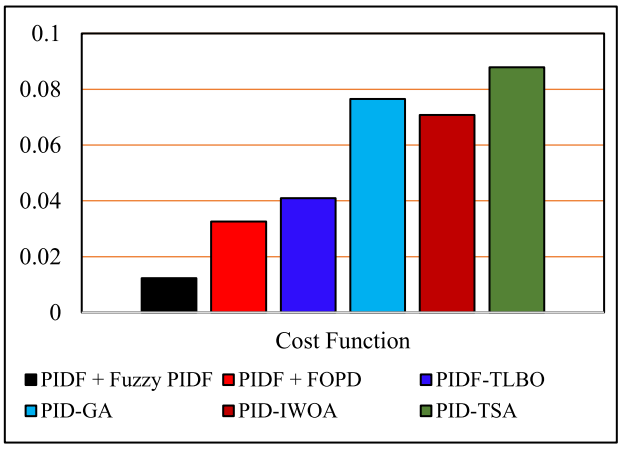

FIGURE 12. The value of ITAE based on different techniques.

of normalized cost function values, while Figures 13 and 14 contrast stability metrics, including maximum percentage overshoot and undershoot (expressed in per unit values), to evaluate transient oscillations. Collectively, these figures provide a rigorous analytical framework for assessing the dynamic responsiveness, optimization efficiency, and

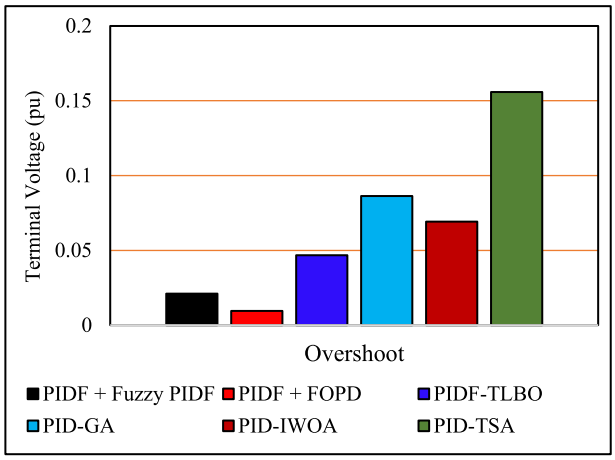

FIGURE 13. The overshoot and undershoot of different techniques.

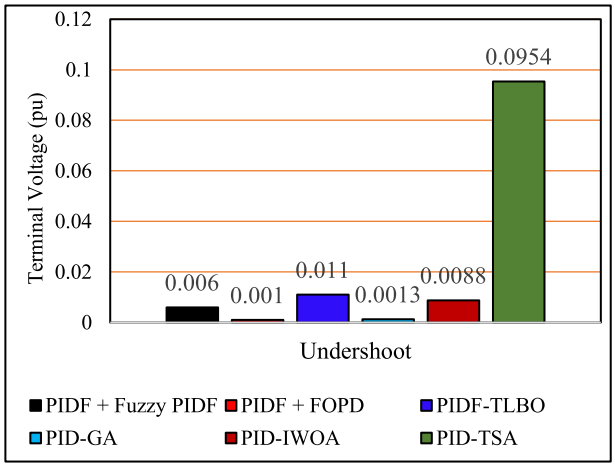

FIGURE 14. The overshoot and undershoot of different techniques.

closed-loop stability of the investigated control paradigms. As evidenced by the empirical data in Figures 10–14 and the statistical synthesis in Table 8, the proposed controller demonstrates superior performance characteristics, achieving enhanced transient stability and accelerated response dynamics relative to established methodologies documented in prior research. The results underscore the controller's success in maintaining voltage regulation precision while exhibiting minimal oscillatory behavior, thereby substantiating its technical viability for deployment in real-world power system applications.

V. ROBUSTNESS ANALYSIS

A. TEST 1: PARAMETRIC UNCERTAINTY ANALYSIS

The inherent susceptibility of system parameters, including gain coefficients and time constants, to continuous variations poses a significant challenge to the operational integrity of closed-loop control systems. Such parametric instabilities can markedly compromise system performance, potentially leading to deviations from desired operational benchmarks. Notably, within the domain of AVR systems, the implications of these parametric uncertainties remain relatively underexplored in the extant literature, underscoring a critical aspect to investigate. This study rigorously examines the systemic repercussions of parameter fluctuations on AVR performance through a methodical analysis of parametric uncertainties. A comprehensive sensitivity assessment is conducted by systematically perturbing each parameter within a ±40% deviation range from its nominal value, thereby evaluating its influence on system stability (Table 9). Furthermore, Figure 15 delineates the destabilizing effects of parametric uncertainties on the AVR system in an uncontrolled configuration, providing empirical insights into the magnitude of performance degradation under such conditions.

TABLE 9. Parametric uncertainty analysis.

Scenario	Nominal	Variation Range	New Value
Generator	K_g=1	+40 % & − 40%	1.4 & 0.6
	τ_g= 1	+40 % & − 40%	1.4 & 0.6
Excitor	K_e=1	+40 % & − 40%	1.4 & 0.6
	τ_e= 0.4	+40 % & − 40%	0.56 & 0.24
Sensor	K_s=1	+40 % & − 40%	1.4 & 0.6
	τ_s= 0.01	+40 % & − 40%	0.014 & 0.006
Amplifier	K_a=10	+40 % & − 40%	14 & 6
	τ_a= 0.1	+40 % & − 40%	0.14 & 0.06
Random critical case	K_g=1	−40%	0.6
	K_e=1	+40%	1.4
	τ_e= 0.4	+40%	0.56
	K_a=10	+40%	14
	τ_a= 0.1	−40%	0.06
	τ_s= 0.01	−40%	0.006

To assess the robustness of the proposed controller, a systematic robustness analysis is performed to evaluate its resilience against parametric uncertainties. Multiple scenarios are evaluated to investigate this aspect. As detailed in Table 9, the controller is subjected to variations in critical parameters, including the Ka, Ke, Tg, and Ts. Additionally, the controller's performance is rigorously examined under a stochastic scenario involving concurrent deviations of multiple parameters from their nominal values, as outlined in Table 9. This multi-parameter perturbation test aims to validate the controller's stability and efficacy in conditions reflecting real-world operational uncertainties. Table 10 and figures 16-20 provide a comparative evaluation of the transient and steady-state operational performance between the hybrid PIFD augmented Fuzzy PIDF controller and a conventional PIDF controller—under varying parametric uncertainty conditions. The results obtained are also compared with a traditional PID-based TSA previously reported in the literature. Critical performance indicators, including peak overshoot, peak undershoot, settling time, rise time and the ITAE, are examined to quantify dynamic responsiveness, stability, and error minimisation capabilities. The analysis contrasts the efficacy of both controllers in mitigating disturbances and maintaining voltage regulation across simulated scenarios characterized by parametric deviations.

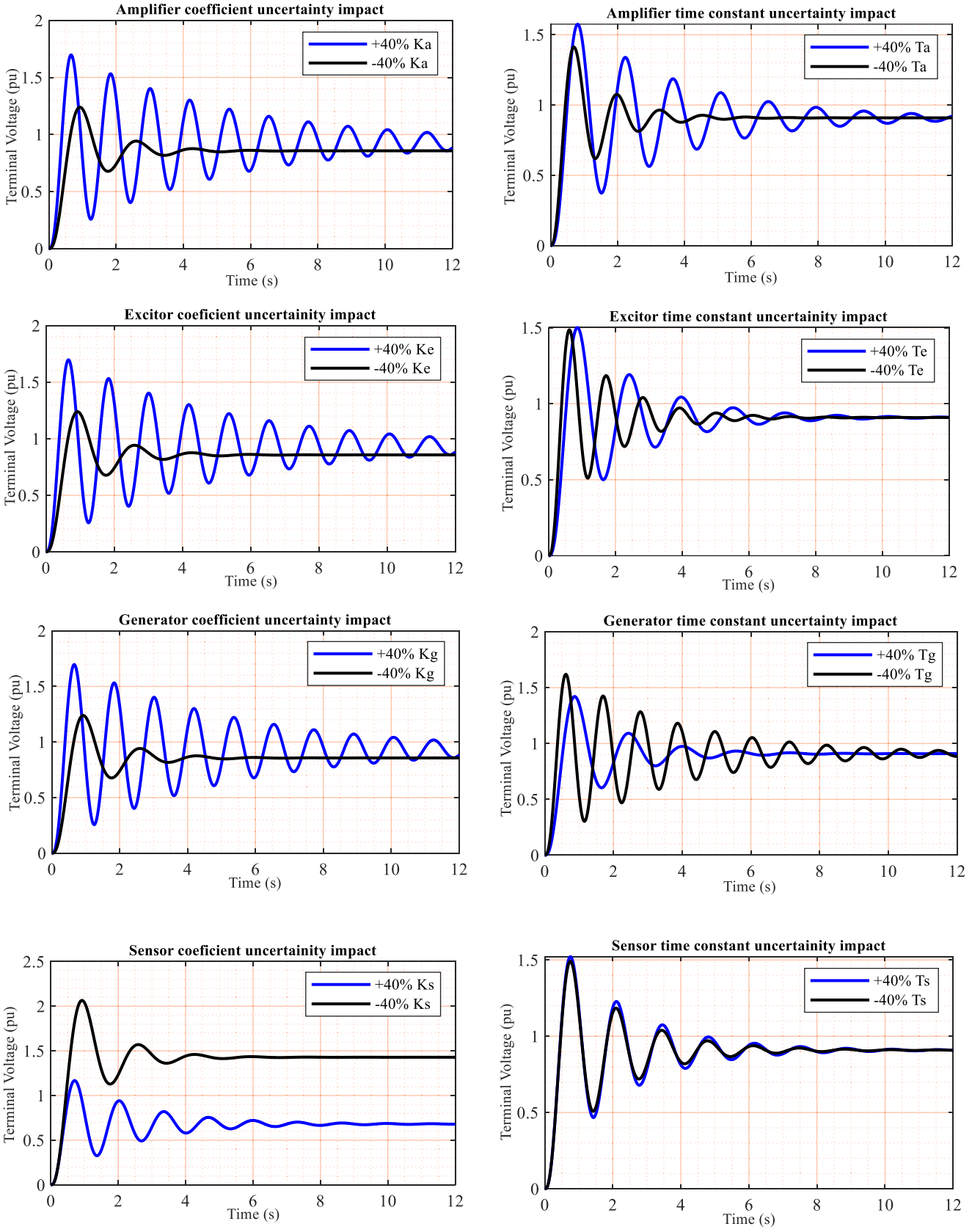

FIGURE 15. The step response of the AVR model with no controller under various parametric uncertainty conditions.

TABLE 10. The performance of two AVR systems under parametric uncertainty conditions.

Controller	POs	PUs	Ts	Tr	ITAE
+40% Ke					
PIDF+Fuzzy PIDF	0.0434	0.008	0.2112	0.1057	0.00816
PIDF:TLBO	0.1202	0.0251	0.9264	0.1988	0.03692
PID: TSA	0.2647	0.138	0.9665	0.1002	0.05932
-40% Ke					
PIDF+Fuzzy PIDF	0.0007	0.0093	0.2979	0.1935	0.02433
PIDF: TLBO	0.0004	0	0.9712	0.5122	0.09014
PID: TSA	0.0141	0.0732	1.1964	0.2174	0.1136
+40% Ka					
PIDF+Fuzzy PIDF	0.0434	0.008	0.2112	0.1057	0.00816
PIDF: TLBO	0.1202	0.0251	0.9264	0.1988	0.03692
PID: TSA	0.2647	0.138	0.9665	0.1002	0.05932
-40% Ka					
PIDF+Fuzzy PIDF	0.0007	0.0093	0.2979	0.1936	0.02433
PIDF: TLBO	0.0004	0	0.9712	0.5122	0.09014
PID: TSA	0.0141	0.0732	1.1964	0.2174	0.1136
+40% Ts					
PIDF+Fuzzy PIDF	0.0436	0.0163	0.2518	0.1270	0.01287
PIDF: TLBO	0.0547	0.01215	0.7405	0.2707	0.04271
PID: TSA	0.1799	0.1072	0.7526	0.1286	0.07553
-40% Ts					
PIDF+Fuzzy PIDF	0.0050	0.0027	0.2026	0.1334	0.01197
PIDF: TLBO	0.0395	0.0101	0.7200	0.2821	0.03941
PID: TSA	0.1344	0.0864	0.7847	0.1349	0.07168
+40% Tg					
PIDF+Fuzzy PIDF	0.0071	0.0050	0.2456	0.1629	0.01771
PIDF: TLBO	0.050	0	1.6538	0.3679	0.1363
PID: TSA	0.0898	0.05132	0.8442	0.1728	0.1126
-40% Tg					
PIDF+Fuzzy PIDF	0.0268	0.01166	0.1849	0.0999	0.01143
PIDF: TLBO	0.0818	0.0731	1.5368	0.1836	0.104
PID: TSA	0.2656	0.1779	1.2857	0.0908	0.06235
Random Scenario					
PIDF+Fuzzy PIDF	0	0	0.2321	0.1331	0.01037
PIDF: TLBO	0.0448	0	1.1428	0.2991	0.5836
PID: TSA	0.0658	0.0385	0.6606	0.1326	0.5914

The PIDF + Fuzzy PIDF controller consistently demonstrates superior performance across all conditions, exhibiting significantly lower overshoot, undershoot, and ITAE values. For instance, with +40% exciter coefficient (Ke) as presented in Figure 16, the Fuzzy controller shows a POs of 0.0434 pu compared to 0.1202 pu for the PIDF based TLBO and 0.2647 PU for PID tuned by TSA, indicating better stability and reduced transient response issues. Notably, the Fuzzy controller achieves a considerably faster settling time (Ts) and rise time (Tr) across these conditions, underscoring its robustness in stabilizing the system quickly. It is also obvious that the impact of the variation of the amplifier coefficient (Ka) is identical to the impact of the variation in the exciter coefficient (Ke) as Figures 16 and 17 demonstrate.

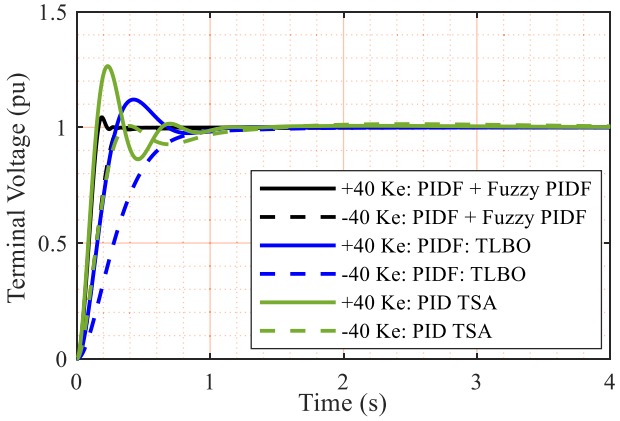

FIGURE 16. Step response curves for variation of Ke.

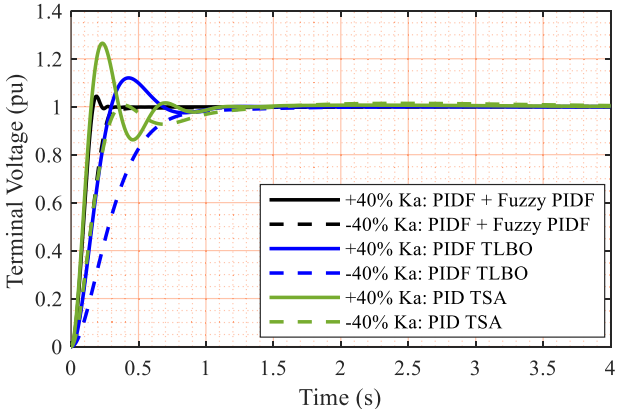

FIGURE 17. Step response curves for variation of Ka.

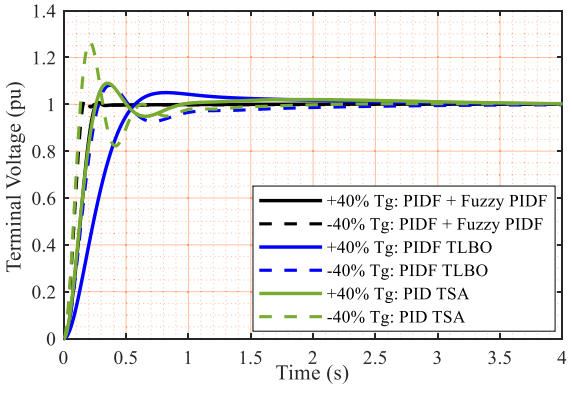

FIGURE 18. Step response curves for variation of Tg.

The Fuzzy PIDF + PIDF controller again exhibits superior transient performance under time-constant Variations (±40% Ts & Tg) with faster response times and reduced error. For instance, as shown in Figure 18, with +40% Tg, the Fuzzy controller's Ts is 0.2456 s compared to the PIDF's 1.6538 s and 0.8442 s for other techniques, highlighting its improved damping capabilities. Also, as given in Figure 19,

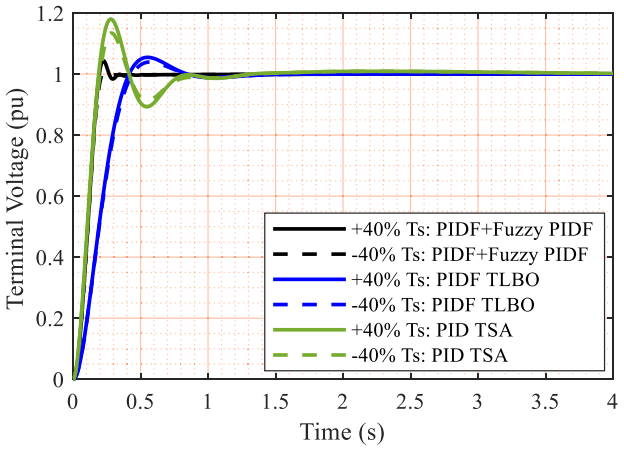

FIGURE 19. Step response curves for variation of Ts.

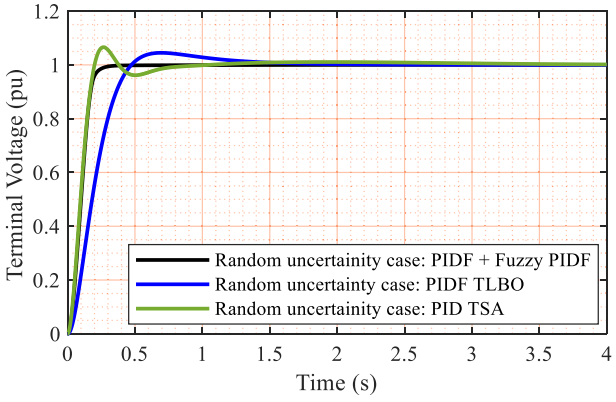

FIGURE 20. Step response curves for variation of a random case.

with −40% Ts, the Fuzzy controller's POs is 0.0050 pu compared to 0.0395 pu and 0.1344 pu based on PIDF based TLBO and PID based on TSA, respectively. showing its improved damping capabilities. The PIDF controller tuned by TLBO and PID based on TSA struggle significantly under these conditions, showing increased oscillations and prolonged stabilization times. However, the classical PIDF controller tuned by TLBO algorithm outperformes the PID based TSA in most cases resulting less overshoot and settling time which reflects a better overall performance.

Figure 20 presents the step response analysis of the AVR model under stochastic parametric uncertainty conditions (presented in Table 9). Despite substantial parametric variations, the system maintained operational stability within predefined acceptable performance boundaries. Notably, the Fuzzy PIDF + PIDF controller, optimized through a two-stage tuning process employing TLBO) and PSO exhibited a marginal reduction in overshoot magnitude. This resulted from the aggregate influence of parametric deviations, which changes the system's effective damping ratio, thereby attenuating the overshoot and undershoot amplitudes. Such stochastic variations emulate realistic operational perturbations that may arise in practical deployment scenarios. The robustness evaluation conclusively demonstrates that the hybrid PIDF and fuzzy PIDF control architecture achieves enhanced reliability and robust performance characteristics, validating its suitability for AVR applications under dynamic and uncertain operating regimes. Moreover, this control approach outperformed the classical PIDF and PID tuned by TLBO and TSA, respectively.

B. TEST2: ROBUSTNESS AGAINST VARYING LOAD CONDITIONS AND CONTROL SIGNAL DISTURBANCES

To evaluate the efficacy of the proposed hybrid PIDF plus Fuzzy PIDF controller, the system was subjected to dynamic load variations and control signal disturbances. Fluctuations in connected electrical loads can induce generator output voltage deviations, presenting a critical challenge to voltage regulation and stability maintenance. Concurrently, control signal disturbances in AVR systems encompass a spectrum of factors, such as sensor inaccuracies, electromagnetic interference, communication errors, component degradation, and control loop instabilities. These disturbances can substantially compromise system performance unless effectively mitigated through robust control design. Consequently, the AVR controller architecture must integrate advanced compensation mechanisms to attenuate such perturbations and ensure operational resilience. These test conditions simulate the most critical operational stressors encountered in real-world power systems, enabling a rigorous assessment of the controller's robustness, adaptability, and dynamic response. The system's block diagram under these disturbances is depicted in Figure 21, illustrating the integration of disturbance models within the AVR framework.

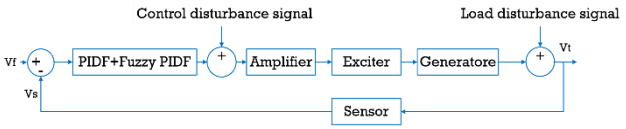

FIGURE 21. The AVR model under load and control signal disturbances.

A notable strength of the controller's robustness lies in its capacity to attenuate the influence of load disturbances on the controlled system. As established in [55], disturbances constituting up to 5% of the generator's output voltage are deemed within tolerable thresholds; nevertheless, controllers must demonstrate proficiency in effectively managing and mitigating disturbances exceeding this benchmark. Consistent with prior methodologies, this study subjected the system to disturbances equivalent to 10% of the reference voltage, introduced directly at the generator's output terminal, to rigorously assess the transient behavior of the system and the controller's disturbance rejection efficacy under heightened operational stress. This approach facilitates a comprehensive evaluation of dynamic performance and validates the controller's capability to maintain stability under extreme perturbation scenarios. Figure 22 illustrates the applied disturbance profiles and corresponding step response characteristics under nominal operating conditions.

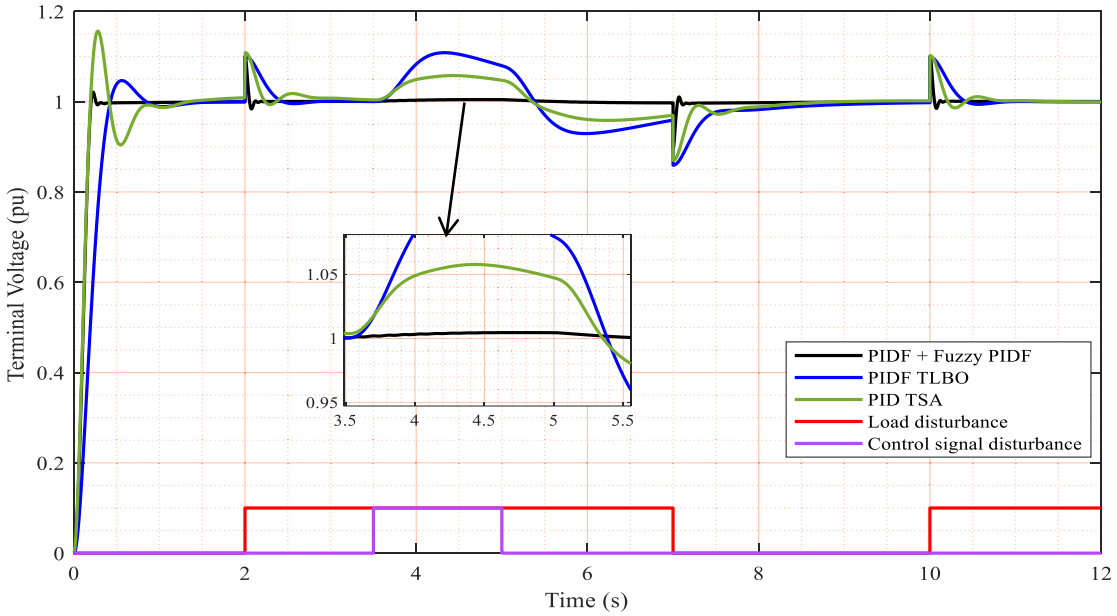

FIGURE 22. The step response of the AVR system under load and control signal disturbances.

The proposed PIDF + Fuzzy PIDF control architecture demonstrates a significant capability in effectively attenuating these disturbances, ensuring consistent system stability and reliable response dynamics across varied operational scenarios. In contrast, the conventional PIDF tuned by TLBO and PID-based TSA controllers exhibit comparatively reduced robustness in mitigating control signal disturbances, highlighting limitations in its adaptability under dynamic conditions. The empirical findings underscore the enhanced robustness of the proposed hybrid controller, affirming its efficacy in addressing stringent operational challenges while maintaining high reliability. These results provide rigorous validation of the controller's capacity to sustain performance integrity in complex control environments.

VI. CONCLUSION AND FUTURE WORK

This study introduces a novel hierarchical control architecture to enhance the reliability and performance of an AVR system. The proposed framework integrates a conventional Proportional-Integral-Derivative with Filter (PIDF) controller with a Fuzzy PIDF-based enhancement mechanism, systematically tuned through a two-stage optimization strategy to ensure operational robustness. In the initial stage, the TLBO is employed to optimize the parameters of the baseline PIDF controller. Subsequently, the PSO algorithm is utilized to refine the Fuzzy PIDF supplementary controller. Crucially, the independent tuning of both components ensures the primary PIDF controller retains full functionality in the event of secondary subsystem failures, thereby guaranteeing system reliability.

Experimental results demonstrate that the hybrid PIDF + Fuzzy PIDF controller achieves superior dynamic performance, including enhanced transient response and steady-state accuracy, outperforming existing control strategies documented in the literature. A rigorous robustness analysis further validates the controller's resilience against parametric uncertainties within the AVR model, as well as external disturbances such as load variations and control signal perturbations. These findings underscore the controller's viability for real-world deployment in critical voltage regulation applications.

Future research directions may explore the integration of advanced control paradigms, such as Sliding Mode Control (SMC) or Model Predictive Control (MPC), as the primary control layer, augmented by adaptive fuzzy or neuro-fuzzy architectures for performance refinement. Additionally, the adoption of alternative metaheuristic optimization techniques or hybrid evolutionary strategies—could further improve parameter tuning efficacy, given its pivotal role in overall control system performance. Such advancements would extend the framework's applicability to complex, nonlinear systems requiring high reliability and adaptability.

Furthermore, while the proposed PIDF + Fuzzy PIDF controller demonstrates exceptional performance in MATLAB/Simulink simulations for AVR systems, future work may focus on bridging the gap between simulation and real-world deployment. Hardware-in-the-Loop (HIL) testing may be conducted to validate the controller's compatibility with physical AVR hardware components, such as exciters, sensors, and microcontrollers.

REFERENCES

[1] M. Furat and G. G. Cücü, "Design, implementation, and optimization of sliding mode controller for automatic voltage regulator system," *IEEE Access*, vol. 10, pp. 55650–55674, 2022, doi: 10.1109/ACCESS.2022.3177621.

[2] M. Z. M. Tumari, M. A. Ahmad, and M. I. Mohd Rashid, "A fractional order PID tuning tool for automatic voltage regulator using marine predators algorithm," *Energy Rep.*, vol. 9, pp. 416–421, Nov. 2023, doi: 10.1016/j.egyr.2023.10.044.

[3] M. Furat, "Chattering attenuation analysis in variable structure control for automatic voltage regulator with input constraints," *Eng. Sci. Technol., Int. J.*, vol. 45, Sep. 2023, Art. no. 101499, doi: 10.1016/j.jestch.2023.101499.

[4] B. K. Dakua, B. Sahoo, and B. B. Pati, "Design of PIλDμ controller for a fractional-order automatic voltage regulator system," *IFAC-PapersOnLine*, vol. 55, no. 1, pp. 649–654, 2022, doi: 10.1016/j.ifacol.2022.04.106.

[5] N. D. Chetty, G. Sharma, R. Gandhi, and E. Çelik, "A novel salp swarm optimization oriented 3-DOF-PIDA controller design for automatic voltage regulator system," *IEEE Access*, vol. 12, pp. 20181–20196, 2024, doi: 10.1109/ACCESS.2024.3360300.

[6] M. Çinar, "Enhancing voltage regulation in synchronous generators: A novel approach with fractional-order PID controllers and wound healing algorithm," *IEEE Access*, vol. 12, pp. 167404–167412, 2024, doi: 10.1109/ACCESS.2024.3496820.

[7] O. M. Hesham, M. A. Attia, and S. F. Mekhamer, "Enhancement of AVR system performance by using hybrid harmony search and dwarf mongoose optimization algorithms," *Sci. Rep.*, vol. 14, no. 1, p. 27177, Nov. 2024, doi: 10.1038/s41598-024-77120-3.

[8] F. Dai and S. Gao, "Optimal design of a PIDD2 controller for an AVR system using hybrid whale optimization algorithm," *IEEE Access*, vol. 12, pp. 128525–128540, 2024, doi: 10.1109/access.2024.3454107.

[9] P. Gopi, S. V. Reddy, M. Bajaj, I. Zaitsev, and L. Prokop, "Performance and robustness analysis of V-Tiger PID controller for automatic voltage regulator," *Sci. Rep.*, vol. 14, no. 1, pp. 1–2, Apr. 2024, doi: 10.1038/s41598-024-58481-1.

[10] A. O. Badr, S. Mansour, M. A. Sameh, and M. A. Attia, "Seamless transition and Fault-Ride-Through by using a fuzzy EO PID controller in AVR system," *Energies*, vol. 15, no. 22, p. 8475, Nov. 2022, doi: 10.3390/en15228475.

[11] E. A. Mohamed, M. Aly, W. Alhosaini, and E. M. Ahmed, "Augmenting the stability of automatic voltage regulators through sophisticated fractional-order controllers," *Fractal Fractional*, vol. 8, no. 5, p. 300, May 2024, doi: 10.3390/fractalfract8050300.

[12] M. Micev, M. Ćalasan, and M. Radulović, "Optimal tuning of the novel voltage regulation controller considering the real model of the automatic voltage regulation system," *Heliyon*, vol. 9, no. 8, Aug. 2023, Art. no. e18707, doi: 10.1016/j.heliyon.2023.e18707.

[13] D. Izci and S. Ekinci, "An improved RUN optimizer based real PID plus second-order derivative controller design as a novel method to enhance transient response and robustness of an automatic voltage regulator," *e-Prime - Adv. Electr. Eng., Electron. Energy*, vol. 2, Jan. 2022, Art. no. 100071, doi: 10.1016/j.prime.2022.100071.

[14] S. M. A. Altbawi, A. S. B. Mokhtar, T. A. Jumani, I. Khan, N. N. Hamadneh, and A. Khan, "Optimal design of fractional order PID controller based automatic voltage regulator system using gradient-based optimization algorithm," *J. King Saud Univ. - Eng. Sci.*, vol. 36, no. 1, pp. 32–44, Jan. 2024, doi: 10.1016/j.jksues.2021.07.009.

[15] P. Shah and S. Agashe, "Review of fractional PID controller," *Mechatronics*, vol. 38, pp. 29–41, Sep. 2016, doi: 10.1016/j.mechatronics.2016.06.005.

[16] S. B. Joseph, E. G. Dada, A. Abidemi, D. O. Oyewola, and B. M. Khammas, "Metaheuristic algorithms for PID controller parameters tuning: Review, approaches and open problems," *Heliyon*, vol. 8, no. 5, May 2022, Art. no. e09399, doi: 10.1016/j.heliyon.2022.e09399.

[17] M. Shouran and M. Alenezi, "Automatic voltage regulator betterment based on a new fuzzy FOPI+FOPD tuned by TLBO," *Fractal Fractional*, vol. 9, no. 1, p. 21, Dec. 2024, doi: 10.3390/fractalfract9010021.

[18] Y. Batmani and H. Golpîra, "Automatic voltage regulator design using a modified adaptive optimal approach," *Int. J. Electr. Power Energy Syst.*, vol. 104, pp. 349–357, Jan. 2019, doi: 10.1016/j.ijepes.2018.07.001.

[19] Ö. Türksoy and A. Türksoy, "A fast and robust sliding mode controller for automatic voltage regulators in electrical power systems," *Eng. Sci. Technol., Int. J.*, vol. 53, May 2024, Art. no. 101697, doi: 10.1016/j.jestch.2024.101697.

[20] S. J. Gambhire, D. R. Kishore, P. S. Londhe, and S. N. Pawar, "Review of sliding mode based control techniques for control system applications," *Int. J. Dyn. Control*, vol. 9, no. 1, pp. 363–378, Mar. 2021, doi: 10.1007/s40435-020-00638-7.

[21] K. J. Åström and T. Hägglund, "The future of PID control," *Control Eng. Pract.*, vol. 9, no. 11, pp. 1163–1175, Nov. 2001.

[22] U. Güvenç, T. YiğiT, A. H. Işik, and I. Akkaya, "Performance analysis of biogeography-based optimization for automatic voltage regulator system," *TURKISH J. Electr. Eng. Comput. Sci.*, vol. 24, no. 3, pp. 1150–1162, 2016, doi: 10.3906/elk-1311-111.

[23] Z.-L. Gaing, "A particle swarm optimization approach for optimum design of PID controller in AVR system," *IEEE Trans. Energy Convers.*, vol. 19, no. 2, pp. 384–391, Jun. 2004, doi: 10.1109/TEC.2003.821821.

[24] Y. O. M. Sekyere, P. O. Ajiboye, F. B. Effah, and B. T. Opoku, "Optimizing PID control for automatic voltage regulators using ADIWACO PSO," *Sci. Afr.*, vol. 27, Mar. 2025, Art. no. e02562, doi: 10.1016/j.sciaf.2025.e02562.

[25] B. Hekimoglu and S. Ekinci, "Grasshopper optimization algorithm for automatic voltage regulator system," in *Proc. 5th Int. Conf. Electr. Electron. Eng. (ICEEE)*, May 2018, pp. 152–156, doi: 10.1109/ICEEE2.2018.8391320.

[26] P. K. Mohanty, B. K. Sahu, and S. Panda, "Tuning and assessment of proportional–integral–derivative controller for an automatic voltage regulator system employing local unimodal sampling algorithm," *Electric Power Compon. Syst.*, vol. 42, no. 9, pp. 959–969, Jul. 2014, doi: 10.1080/15325008.2014.903546.

[27] B. K. Sahu, S. Panda, P. K. Mohanty, and N. Mishra, "Robust analysis and design of PID controlled AVR system using pattern search algorithm," in *Proc. IEEE Int. Conf. Power Electron., Drives Energy Syst. (PEDES)*, Dec. 2012, pp. 1–6, doi: 10.1109/PEDES.2012.6484294.

[28] H. Gozde and M. C. Taplamacioglu, "Comparative performance analysis of artificial bee colony algorithm for automatic voltage regulator (AVR) system," *J. Franklin Inst.*, vol. 348, no. 8, pp. 1927–1946, Oct. 2011, doi: 10.1016/j.jfranklin.2011.05.012.

[29] B. Hekimoğlu, "Sine-cosine algorithm-based optimization for automatic voltage regulator system," *Trans. Inst. Meas. Control*, vol. 41, no. 6, pp. 1761–1771, Apr. 2019, doi: 10.1177/0142331218811453.

[30] S. Panda, B. K. Sahu, and P. K. Mohanty, "Design and performance analysis of PID controller for an automatic voltage regulator system using simplified particle swarm optimization," *J. Franklin Inst.*, vol. 349, no. 8, pp. 2609–2625, Oct. 2012, doi: 10.1016/j.jfranklin.2012.06.008.

[31] S. Habib, G. Abbas, T. A. Jumani, A. A. Bhutto, S. Mirsaeidi, and E. M. Ahmed, "Improved whale optimization algorithm for transient response, robustness, and stability enhancement of an automatic voltage regulator system," *Energies*, vol. 15, no. 14, p. 5037, Jul. 2022, doi: 10.3390/en15145037.

[32] E. Köse, "Optimal control of AVR system with tree seed algorithm-based PID controller," *IEEE Access*, vol. 8, pp. 89457–89467, 2020, doi: 10.1109/ACCESS.2020.2993628.

[33] E. Çelik and R. Durgut, "Performance enhancement of automatic voltage regulator by modified cost function and symbiotic organisms search algorithm," *Eng. Sci. Technol., Int. J.*, vol. 21, no. 5, pp. 1104–1111, Oct. 2018, doi: 10.1016/j.jestch.2018.08.006.

[34] P. Gopi, M. Mahdavi, and H. Haes Alhelou, "Robustness and stability analysis of automatic voltage regulator using disk-based stability analysis," *IEEE Open Access J. Power Energy*, vol. 10, pp. 689–700, 2023, doi: 10.1109/OAJPE.2023.3344750.

[35] N. Razmjooy, M. Khalilpour, and M. Ramezani, "A new meta-heuristic optimization algorithm inspired by FIFA world cup competitions: Theory and its application in PID designing for AVR system," *J. Control, Autom. Electr. Syst.*, vol. 27, no. 4, pp. 419–440, Aug. 2016, doi: 10.1007/s40313-016-0242-6.

[36] Y. Zhou, J. Zhang, X. Yang, and Y. Ling, "Optimization of PID controller based on water wave optimization for an automatic voltage regulator system," *Inf. Technol. Control*, vol. 48, no. 1, pp. 162–169, Mar. 2019, doi: 10.5755/j01.itc.48.1.20296.

[37] A. M. Mosaad, M. A. Attia, and A. Y. Abdelaziz, "Whale optimization algorithm to tune PID and PIDA controllers on AVR system," *Ain Shams Eng. J.*, vol. 10, no. 4, pp. 755–767, Dec. 2019, doi: 10.1016/j.asej.2019.07.004.

[38] A. M. Mosaad, M. A. Attia, and A. Y. Abdelaziz, "Comparative performance analysis of AVR controllers using modern optimization techniques," *Electric Power Compon. Syst.*, vol. 46, nos. 19–20, pp. 2117–2130, Dec. 2018, doi: 10.1080/15325008.2018.1532471.

[39] B. Ozgenc, M. S. Ayas, and I. H. Altas, "Performance improvement of an AVR system by symbiotic organism search algorithm-based PID-F controller," *Neural Comput. Appl.*, vol. 34, no. 10, pp. 7899–7908, May 2022, doi: 10.1007/s00521-022-06892-4.

[40] M. A. Sahib, "A novel optimal PID plus second order derivative controller for AVR system," *Eng. Sci. Technol., Int. J.*, vol. 18, no. 2, pp. 194–206, Jun. 2015, doi: 10.1016/j.jestch.2014.11.006.
[41] Y. Li, L. Ni, G. Wang, S. S. Aphale, and L. Zhang, "Q-learning-based dumbo octopus algorithm for parameter tuning of fractional-order PID controller for AVR systems," *Mathematics*, vol. 12, no. 19, p. 3098, Oct. 2024, doi: 10.3390/math12193098.
[42] M. Micev, M. Ćalasan, and D. Oliva, "Fractional order PID controller design for an AVR system using chaotic yellow saddle goatfish algorithm," *Mathematics*, vol. 8, no. 7, p. 1182, Jul. 2020, doi: 10.3390/math8071182.
[43] M. Z. Mohd Tumari, M. A. Ahmad, M. H. Suid, and M. R. Hao, "An improved marine predators algorithm-tuned fractional-order PID controller for automatic voltage regulator system," *Fractal Fractional*, vol. 7, no. 7, p. 561, Jul. 2023, doi: 10.3390/fractalfract7070561.
[44] S. Ekinci, V. Snášel, R. M. Rizk-Allah, D. Izci, M. Salman, and A. A. F. Youssef, "Optimizing AVR system performance via a novel cascaded RPIDD2-FOPI controller and QWGBO approach," *PLoS ONE*, vol. 19, no. 5, May 2024, Art. no. e0299009, doi: 10.1371/journal.pone.0299009.
[45] A. Tabak, "Modified and improved TID controller for automatic voltage regulator systems," *Fractal Fractional*, vol. 8, no. 11, p. 654, Nov. 2024, doi: 10.3390/fractalfract8110654.
[46] S. Ekinci, H. Çetin, D. Izci, and E. Köse, "A novel balanced arithmetic optimization algorithm-optimized controller for enhanced voltage regulation," *Mathematics*, vol. 11, no. 23, p. 4810, Nov. 2023, doi: 10.3390/math11234810.
[47] A. Tabak, "Novel TIλDND2N2 controller application with equilibrium optimizer for automatic voltage regulator," *Sustainability*, vol. 15, no. 15, p. 11640, Jul. 2023, doi: 10.3390/su151511640.
[48] A. Idir, L. Canale, Y. Bensafia, and K. Khettab, "Design and robust performance analysis of low-order approximation of fractional PID controller based on an IABC algorithm for an automatic voltage regulator system," *Energies*, vol. 15, no. 23, p. 8973, Nov. 2022, doi: 10.3390/en15238973.
[49] A. Laib, B. Talbi, A. Krama, and M. Gharib, "Hybrid interval type-2 fuzzy PID+I controller for a multi-DOF oilwell drill-string system," *IEEE Access*, vol. 10, pp. 67262–67275, 2022, doi: 10.1109/ACCESS.2022.3185021.
[50] A. Kumar and V. Kumar, "Performance analysis of optimal hybrid novel interval type-2 fractional order fuzzy logic controllers for fractional order systems," *Expert Syst. Appl.*, vol. 93, pp. 435–455, Mar. 2018, doi: 10.1016/j.eswa.2017.10.033.
[51] A. Laib and M. Gharib, "Design of an intelligent cascade control scheme using a hybrid adaptive neuro-fuzzy PID controller for the suppression of drill string torsional vibration," *Appl. Sci.*, vol. 14, no. 12, p. 5225, Jun. 2024, doi: 10.3390/app14125225.
[52] R. V. Rao, V. J. Savsani, and D. P. Vakharia, "Teaching–Learning-Based optimization: An optimization method for continuous non-linear large scale problems," *Inf. Sci.*, vol. 183, no. 1, pp. 1–15, Jan. 2012, doi: 10.1016/j.ins.2011.08.006.
[53] M. F. Aranza, J. Kustija, B. Trisno, and D. L. Hakim, "Tunning PID controller using particle swarm optimization algorithm on automatic voltage regulator system," *IOP Conf., Mater. Sci. Eng.*, vol. 128, May 2016, Art. no. 012038, doi: 10.1088/1757-899x/128/1/012038.
[54] M. Shouran and A. Alsseid, "Particle swarm optimization algorithm-tuned fuzzy cascade fractional order PI-fractional order PD for frequency regulation of dual-area power system," *Processes*, vol. 10, no. 3, p. 477, Feb. 2022, doi: 10.3390/pr10030477.
[55] M. Shouran, M. Alenezi, M. N. Muftah, A. Almarimi, A. Abdallah, and J. Massoud, "A novel AVR system utilizing fuzzy PIDF enriched by FOPD controller optimized via PSO and sand cat swarm optimization algorithms," *Energies*, vol. 18, no. 6, p. 1337, Mar. 2025, doi: 10.3390/en18061337.

MOKHTAR SHOURAN received the B.Sc. degree in control engineering from the College of Electronic Technology, Bani Waled, Libya, in 2011, the M.Sc. degree in electronics and information technology from the University of South Wales, Treforest, U.K., in 2017, and the Ph.D. degree in power systems stability and control from the School of Engineering, Cardiff University, Cardiff, U.K., in 2023. He is currently a Senior Researcher with Libyan Centre for Engineering Research and Information Technology, Bani Walid. His research interests include optimization algorithms, fuzzy logic control, sliding mode control, traditional control, power system stability, and robotics.

MOHAMMED ALENEZI received the degree in electrical and electronics engineering, the Bachelor of Science degree in electrical and electronics engineering from the University of Huddersfield, in 2020, and the Master of Science degree in electrical and electronics engineering from Bangor University, in 2021. He is currently pursuing the Ph.D. degree with Cardiff University, where his research interests include optimization algorithms, machine learning, fault diagnosis, and power system stability and control.